


Article

Evaluation of the Molecular Conformation of Surface Alkyl Chains of Alkylsilane-Derived Hybrid Films Using Sum-Frequency Generation Spectroscopy

Rika Mizuno ¹, Chihiro Urata ², Ken Watanabe ², Atsushi Hozumi ² and Takayuki Miyamae ^{1,*} 
¹ Graduate School of Engineering, Chiba University, Chiba 263-8522, Japan; rikarika3269@gmail.com

² Innovative Functional Materials Research Institute, National Institute of Advanced Industrial Science and Technology (AIST), Nagoya 463-8560, Japan; chihiro-urata@aist.go.jp (C.U.); nabew.nabek19@gmail.com (K.W.); a.hozumi@aist.go.jp (A.H.)

* Correspondence: t-miyamae@chiba-u.jp

Abstract: Alkylsilane-derived hybrid films exhibiting excellent dynamic dewetting behaviors toward various liquids are promising, since they are smooth, highly transparent, and a low environmental burden. However, the detailed mechanism of their unique dynamic dewetting behaviors and its relation to the surface segregation of alkylsilanes during the film formation have not yet been clearly identified. In this study, we prepared various hybrid films by varying the mixing ratios of tetraethoxysilane (TEOS) and *n*-dodecyltriethoxysilane (C12TES) and investigated the changes in the s-CH₂/s-CH₃ peak strength ratios of the resulting hybrid films under dry and wet conditions by sum-frequency generation (SFG) spectroscopy. When the static/dynamic water contact angles significantly changed, it was clearly observed that the s-CH₂/s-CH₃ ratio of each hybrid film under dry and wet condition also changed markedly. With increasing TEOS concentration, the static contact angles became smaller, while the contact angle hysteresis tended to increase because of the increase in gauche defects at the air interface and hydrogen bonds. This finding suggests that the concentration and conformation of the alkyl chains derived from surface-segregated C12TES molecules play an important role in determining the final dewetting behaviors of the hybrid films to water.

Keywords: SFG; liquid-repellent surfaces; water contact angle; dewetting



Citation: Mizuno, R.; Urata, C.; Watanabe, K.; Hozumi, A.; Miyamae, T. Evaluation of the Molecular Conformation of Surface Alkyl Chains of Alkylsilane-Derived Hybrid Films Using Sum-Frequency Generation Spectroscopy. *Solids* **2022**, *3*, 147–154. <https://doi.org/10.3390/solids3010010>

Academic Editor: Maija Nissinen

Received: 28 February 2022

Accepted: 15 March 2022

Published: 17 March 2022

Publisher's Note: MDPI stays neutral with regard to jurisdictional claims in published maps and institutional affiliations.



Copyright: © 2022 by the authors. Licensee MDPI, Basel, Switzerland. This article is an open access article distributed under the terms and conditions of the Creative Commons Attribution (CC BY) license (<https://creativecommons.org/licenses/by/4.0/>).

1. Introduction

The development of simple and durable liquid-repellent surfaces has attracted increasing attention lately, especially in the field of coating applications [1,2]. Many efforts have thus far been made to prepare omniphobic surfaces that can repel not only water but also various other liquids, such as oils and organic solvents [3–8]. For this purpose, alkylsilane-derived hybrid films that exhibit excellent dynamic dewetting behaviors toward various liquids are promising, since they offer the practical advantages of smooth, highly transparent, and low environmental burden [3]. To elucidate the detailed mechanism of the unique dynamic dewetting behaviors of alkylsilane-derived hybrid films, it is crucial to understand the detailed conditions of the alkylsilanes during the film formation. However, the relationship between the dynamic reorientation behaviors of alkylsilanes and their surface segregation state during the film formation has not yet been clearly identified.

Our previous studies have revealed that contacting liquids having different dielectric constants strongly influence the conformation state of the alkyl chains tethered to the hybrid film surfaces, and such conformational changes of alkyl chains also affect the final dynamic dewetting properties of the hybrid films [3]. It is known that infrared-visible sum-frequency generation (SFG) spectroscopy is a very powerful technique to study the conformational changes of the molecules at the surface and/or interface. SFG is a spectroscopic technique that utilizes second-order nonlinear optical effects. Although

isotropic medium such as glass is SFG-inactive in the bulk due to its inversion center [9–11], the symmetry is broken at the interface between two isotropic media with different dielectric constants and SFG becomes active. SFG is resonantly enhanced when the incident infrared frequency overlaps with the resonant frequency of a molecular vibrational mode that is both infrared and Raman active. Therefore, SFG spectroscopy is a surface- and interface-specific vibrational spectroscopic technique that can be used to investigate the molecular orientation, aggregation, and segregation of the molecules at the surface and/or interface with high specificity in situ.

In this study, tetraethoxysilane (TEOS) and *n*-dodecyltriethoxysilane (C12TES) were selected to prepare a model alkylsilane-derived hybrid film. We used SFG to investigate the changes in the molecular conformations of the hybrid film surfaces, which were prepared by varying the mixing ratios of [TEOS]/[C12TES], under dry and wet conditions. We also carried out static and dynamic water contact angle (CA) measurements and investigated the relationship between the final dewetting properties and the surface segregation of the alkylsilane molecules in the topmost region close to the hybrid film surfaces. Marked changes in the SFG peak strength ratios between the dry and wet conditions of each hybrid film were clearly observed when the static/dynamic water CAs changed significantly. This result suggests that the surface segregation behaviors of C12TES molecules during the film formation may play an important role in determining the final water dewetting behaviors of the hybrid films.

2. Materials and Methods

2.1. Materials

Ethanol (EtOH, 99.5+%), deuterium oxide (D₂O, 99 atom%D), and 0.01 M hydrochloric acid (HCl) were purchased from Wako Pure Chemical Industries Ltd (Osaka, Japan). Tetraethoxysilane (TEOS) and *n*-dodecyltriethoxysilane (C12TES) were purchased from Tokyo Kasei Kogyo. Co., Ltd. (Tokyo, Japan). All chemicals were used as received.

2.2. Alkylsilane-Derived Hybrid Film

The C12TES/TEOS hybrid films were prepared using a conventional cohydrolysis and co-condensation method according to previous reports [3,12,13]. Precursor solutions were prepared by mixing C12TES and TEOS in an ethanol/hydrochloric acid solution for 24 h at room temperature (25 ± 2 °C). The molar ratios of precursor compounds are listed in Table 1. This precursor solution was then spin-coated (2000 rpm for 10 s) onto UV-ozone-cleaned water-free synthetic fused silica plates (ϕ 30 mm \times thickness 3 mm, Sigmakoki Co., Ltd. Tokyo, Japan) and glass slides (76 mm \times 26 mm, thickness 1 mm for contact angle measurements) at room temperature and under a relative humidity of $40 \pm 5\%$ to yield hybrid thin films. These hybrid films were then dried in air at room temperature for more than 24 h. The thickness of the hybrid films used in this study was about 100 nm. When the hybrid samples had high C12TES ratios (#1 and #2), many cracks were observed on their surfaces, resulting in roughened and frosted appearances. However, when the values of the [TEOS]/[C12TES] ratio was 9.1 (#3) or higher, the hybrid films were transparent and flat.

2.3. The Static/Dynamic Water Contact Angles

The static/dynamic water CAs were measured using CA goniometers (Kyowa Interface Science, Saitama, Japan, Model DH501Hi for static CA measurements and model CA-V150 for advancing and receding CA measurements). The static CAs were collected using 3 μ L of probe water at 25 °C. For dynamic CA measurements, approximately 3 μ L of water droplet was added and withdrawn from the surface.

Table 1. The molar ratios of precursor compounds of the alkylsilane-derived hybrid films.

Sample No.	TEOS (mmol)	C12TES (mmol)	[TEOS]/[C12TES]	Water (mmol)	EtOH (mmol)
#1	1.7	1.7	1	44	69
#2	3.1	8.3×10^{-1}	3.7	44	69
#3	3.8	4.2×10^{-1}	9.1	44	69
#4	4.1	2.1×10^{-1}	2.0×10^1	44	69
#5	4.3	1.0×10^{-1}	4.1×10^1	44	69
#6	4.4	5.2×10^{-2}	8.5×10^1	44	69
#7	4.4	2.6×10^{-2}	1.7×10^2	44	69
#8	4.5	1.3×10^{-2}	3.4×10^2	44	69
#9	4.5	6.5×10^{-3}	6.9×10^2	44	69
#10	4.5	3.2×10^{-3}	1.4×10^3	44	69
#11	4.5	1.6×10^{-3}	2.8×10^3	44	69
#12	4.5	8.1×10^{-4}	5.5×10^3	44	69
#13	4.5	4.1×10^{-4}	1.1×10^4	44	69
#14	4.5	2.0×10^{-4}	2.2×10^4	44	69
#15	4.5	1.0×10^{-4}	4.4×10^4	44	69
#16	4.5	5.1×10^{-5}	8.8×10^4	44	69
#17	4.5	2.5×10^{-5}	1.8×10^5	44	69
#18	4.5	1.3×10^{-5}	3.5×10^5	44	69
#19	4.5	6.3×10^{-6}	7.1×10^5	44	69
#20	4.5	3.2×10^{-6}	1.4×10^6	44	69

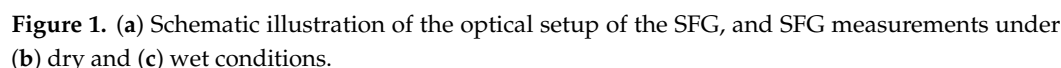
2.4. Sum-Frequency Generation (SFG) Spectroscopy

The details of the SFG system shown in Figure 1a utilized in this study have been reported previously [3,14]. In this experiments, the main laser source was employed a mode-locked Nd:YAG laser with a 1.06 nm wavelength, 130 mJ pulse energy, and 25 ps pulse width (PL2251-C, Ekspla, Vilnius, Lithuania), operating at a repetition rate of 10 Hz. This laser pump beam provided an optical parametric/difference frequency generation system (PG401 VIR/DFG, Ekspla, Vilnius, Lithuania) to produce an IR output that was tunable from 2.5 to 10 μm with a 300 μJ pulse energy. The tunable IR beam was overlapped with a frequency-doubled output of 532 nm from the laser at the sample surface with spatial and temporal incidence angles of 50° and 70°, respectively. Typical spectral resolution of IR is around 6 cm^{-1} . Data were collected in 3 cm^{-1} increments in the region from 2800 to 3000 cm^{-1} , and the data were averaged over 150 laser shots per points. The SFG spectra were normalized for IR and visible intensity variations. In this study, SFG spectra were measured at the air-hybrid film and the D₂O-hybrid film interfaces, respectively. In the SFG measurement of the D₂O-hybrid film interface, the hybrid film-coated side of the quartz substrate was placed in contact with D₂O and laser beams were incident through the transparent substrate. The sample set-up of the SFG experiments under dry and wet conditions is shown in Figure 1.

The SFG output frequency $\omega_{\text{SFG}} = \omega_{\text{VIS}} + \omega_{\text{IR}}$ was generated at the overlapping beam area of both the incident beams, an IR beam of frequency ω_{IR} and a visible beam of frequency ω_{VIS} . The intensity of the SFG output I_{SFG} can be expressed as:

$$I_{\text{SFG}} \propto \left| P^{(2)}(\omega_{\text{SFG}}) \right|^2 = \left| \chi_{\text{NR}}^{(2)} + \sum_v \frac{\chi_v}{\omega_{\text{IR}} - \omega_v + i\Gamma_v} \right|^2 \quad (1)$$

where χ_v , ω_v , and Γ_v are the strength, resonance frequency, and damping coefficient, respectively, of the v -th vibrational mode. $\chi_{\text{NR}}^{(2)}$ describes the non-resonant contribution to the nonlinear susceptibility, which contributes to the background signal and does not depends on the IR frequency [15].



Static water CAs and CA hysteresis (difference between advancing and receding CAs) of the hybrid films prepared by varying the [TEOS]/[C12TES] mixing ratios were summarized in Figure 2. As can be seen, the static CAs of the hybrid films are classified into three major regions depending on the mixing ratios of [TEOS]/[C12TES]. In the first region, the changes in static water CAs did not show a linear relationship to the mixing ratios of [TEOS]/[C12TES], and the initial values remained almost unchanged even after 690-times dilution with TEOS (#9). In the second region, rapid changes in the static CAs are observed in the interval from #9 to #14. Then, static water CAs became almost identical (about $53 \pm 3^\circ$) to that of the TEOS-only film when the TEOS concentrations were high (#15–#20).

Figure 1 is a plot showing the relationship between the θ_s (left y-axis, 40 to 120 degrees) and $\Delta\theta$ (right y-axis, 0 to 20 degrees) versus the $[\text{TEOS}]/[\text{C12TES}]$ ratio (x-axis, logarithmic scale from 10^0 to 10^6). The plot displays data points for various samples, labeled #3, #9, #13, and #20. Open circles represent θ_s values, and filled circles represent $\Delta\theta$ values. Arrows indicate the mapping of θ_s to $\Delta\theta$ for specific points.

Figure 2. Changes in the static water CAs (θ_s , open circle) and CA hysteresis ($\Delta\theta$, filled circle) of the hybrid films as a function of the [TEOS]/[C12TES] molar ratios. [TEOS]/[C12TES] ratios = 9.1 (#3), 690 (#9), 11,000 (#13), 1,400,000 (#20).

To obtain detailed information on the molecular conformation of the hybrid film surfaces, the SFG spectroscopy under dry (air/hybrid film interfaces) and wet (D_2O /hybrid film interfaces) conditions were demonstrated. Figure 3a,b show the SSP-polarized (i.e., S-polarized SFG beam, S-polarized visible beam, and P-polarized IR beam) SFG spectra of the hybrid films in the C–H stretching region ($2800\text{--}3000\text{ cm}^{-1}$) under dry and wet conditions, respectively. Peaks at 2882 cm^{-1} , 2855 cm^{-1} , and 2945 cm^{-1} correspond to the symmetric stretching of the methyl ($s\text{-CH}_3$, r^+), symmetric stretching of methylene ($s\text{-CH}_2$, d^+), and Fermi resonance (FR) of the methyl groups, respectively [15–17]. In the case of the higher C12TES concentrations (#3 and #6), almost no CH_2 peaks were observed in the SFG spectra collected under dry condition, while they were clearly detected on the hybrid films with higher TEOS concentrations (#9–#14). The absence of the CH_2 peaks indicates that the alkyl chains have an all-trans and standing-up configuration at the surface, while the presence of the CH_2 peaks indicates that the gauche defects in the alkane chains are introduced [18–22]. Thus, in the case of hybrid films #3 and #6, highly ordered hybrid films with negligible gauche defects were expected to be formed.

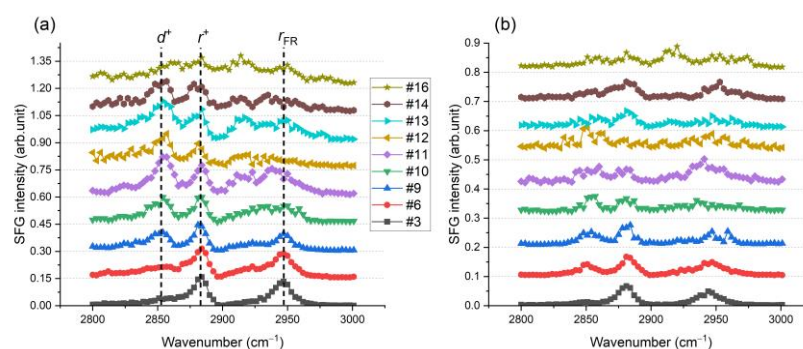


Figure 3. SFG spectra of the hybrid films under (a) dry and (b) wet conditions (SSP). The intensities of the whole SFG spectra are normalized by the intensities of the peak at 2882 cm^{-1} of the symmetric stretching of the methyl group (r^+) and are offset upward for clarity.

When the hybrid films were in contact with water (Figure 3b), marked changes in the SFG spectra in CH stretching region, as compared with those in the dry state, were observed. Although, in the case of hybrid films #3 and #16, there were no significant differences between dry and wet conditions, the difference in the relative intensities of the r^+ and d^+ of the SFG spectra under wet conditions seem to be different from those under dry conditions with increasing TEOS concentration, especially for the hybrid films from #10 to #14. To investigate the conformation of the surface-tethered alkyl chains and their reorientation behaviors in contact with water, the relative peak strength ratios (d^+/r^+) were plotted as a function of the $[\text{TEOS}]/[\text{C12TES}]$ molar ratios (Figure 4). In order to contrast with the changes in static contact angles, we also depicted the static contact angle data shown in Figure 2. As shown, the d^+/r^+ ratios evaluated from the SFG spectra collected under dry conditions gradually increased with increasing TEOS concentration. The d^+/r^+ ratio reached its maximum at #13 where the static CA also changed significantly, and then decreased with further increasing TEOS concentration. Although the change in d^+/r^+ ratios showed a similar trend between the wet and dry conditions, the values of the d^+/r^+ ratios obtained under wet conditions were different from those under dry conditions for each film, suggesting that the molecular orientation of the alkyl chains changed upon contact with water. According to our previous studies, at the *n*-decyltriethoxysilane (C10TES)/tetramethoxysilane (TMOS) hybrid film interfaces, reorientation behaviors of alkyl chains were similarly observed [3]. In this case, molecular orientation of the alkyl chains changed in order to reduce the surface free energy gap with water, resulting in the preferential appearance of many gauche defects at the water interface. However, in our present case, gauche defects were detected even at the air interface, and they decreased when the film surfaces were contacted with water. This was

probably due to the difference in the total amount of alkyl chains existing on the sample surfaces. Although our previous C10TES/TMOS hybrid films were fabricated with a molar ratio of $[\text{TMOS}]/[\text{C10TES}] = 4:1$, the present $[\text{TEOS}]/[\text{C12TES}]$ hybrid films showing more gauche defects were prepared with much higher TEOS concentrations. Thus, the alkyl chains on the surfaces may have a disordered structure even at the air interface. In other words, at the higher TEOS concentrations, C12TES may be segregated on the surface but randomly oriented.

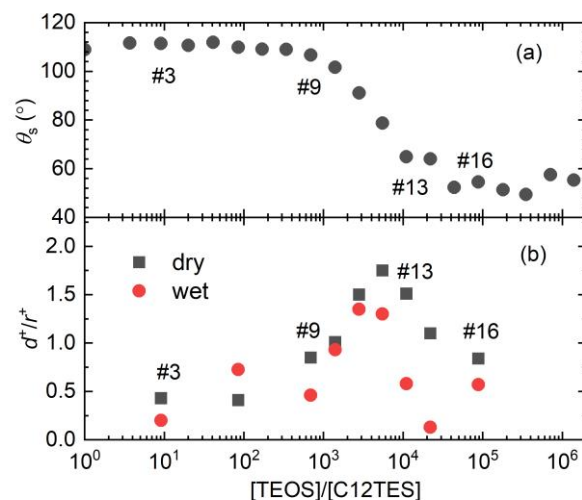


Figure 4. Changes in the (a) static water CAs and (b) $s\text{-CH}_2/s\text{-CH}_3$ ratios of the hybrid films under dry and wet conditions as a function of the $[\text{TEOS}]/[\text{C12TES}]$ molar ratios. $[\text{TEOS}]/[\text{C12TES}]$ ratios = 9.1 (#3), 690 (#9), 11,000 (#13), 88,000 (#16).

This hypothesis can be confirmed by comparing the intensities of the SFG spectra of the sample surfaces with and without C12TES. In Figure 5, typical SFG spectra of the hybrid film surfaces of $[\text{TEOS}]/[\text{C12TES}] = 9.1$ (#3), 5500 (#12), and a TEOS-only film surface were shown. As can be seen, the intensity of the SFG spectrum of the hybrid film #12 (high molar TEOS concentration) was much weaker than that of #3 (low molar TEOS concentration), indicating that the surface alkyl chains had a rather random structure. Furthermore, the SFG spectrum of the TEOS-only film surface showed almost no peaks, indicating that the ethoxy groups of TEOS dissociated completely and hardly remained on the surface in the air.

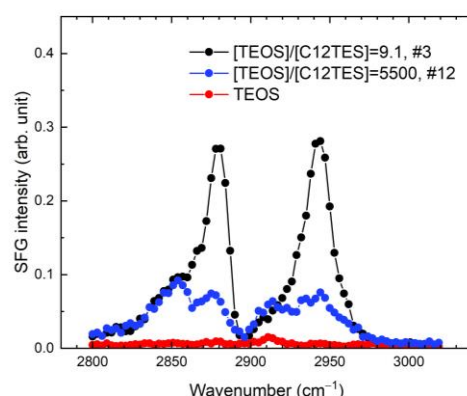


Figure 5. SSP-polarized SFG spectra of the hybrid film surfaces of $[\text{TEOS}]/[\text{C12TES}] = 9.1$ (#3), 5500 (#12), and TEOS-only film under dry conditions.

Based on the above discussions, the reorientation behaviors of alkyl chains on the hybrid film surfaces prepared with relatively higher TEOS concentrations in contact with water can be explained as follows. In these cases, the alkyl chains are considered to be

segregated at the film surfaces, but they are not densely packed, even at the air interface, resulting in the formation of gauche defects. In addition, the ethoxy groups of TEOS were almost completely dissociated and then became hydrophilic parts (Si-OH). When water comes in contact with such surfaces, water molecules tend to not only interact with the hydrophilic parts but also penetrate into the alkyl chains, leading to the reorientation of the residual alkyl chains on the surfaces from a disordered structure to a slightly ordered structure. However, judging from the CA hysteresis shown in Figure 2, the former effect seems to be primarily dominated. As can be seen, CA hysteresis gradually increased with increasing TEOS concentration and remained almost unchanged over the hybrid films #13. This was probably due to the increase in the interaction between water and hydrophilic parts of the surfaces through the hydrogen bonds. These results suggest that the concentration of surface-segregated C12TES molecules may play an important role in determining the final static/dynamic water dewettability of the hybrid films. Although the hybrid films were formed by co-hydrolysis and co-condensation method from the precursor solutions, it can be concluded that the initial molar ratio of the precursor solution and the final composition of the resulting hybrid surface did not necessarily match [23,24].

4. Conclusions

We investigated the relation between the static/dynamic dewettability of the alkylsilane-derived hybrid film surfaces and their surface structures by using static and dynamic contact angle measurements and SFG spectroscopy. In this study, model hybrid film surfaces were prepared by varying the [TEOS]/[C12TES] mixing ratios. With increasing TEOS concentration, the static contact angles (CAs) became small. In addition, based on the relative peak strength ratios ($d^+(s\text{-CH}_2)/r^+(s\text{-CH}_2)$) observed in SFG, the alkyl chains were considered to be segregated at the film surfaces and preferentially formed gauche defects at the higher TEOS concentrations, leading to an increase in CA hysteresis. On further increasing TEOS concentration, the reorientation of the residual alkyl chains on the surfaces from a disordered structure to a slightly ordered structure upon contact with water could be confirmed. However, in this case, water may preferentially interact with the hydrophilic parts derived from the dissociation of ethoxy groups of TEOS, resulting in the further increase in CA hysteresis due to the hydrogen bonds. Therefore, the concentration of surface-segregated C12TES molecules and the conformation of their alkyl chains may play an important role in determining the final surface static and dynamic wetting behaviors of the alkylsilane-derived hybrid films. In the near future, we plan to report on the changes in molecular orientation of the alkylsilane-derived hybrid films upon contact with other probe liquids.

Author Contributions: Conceptualization, T.M., A.H. and C.U.; formal analysis, R.M. and T.M.; Sample preparation, C.U., K.W. and A.H.; writing—original draft preparation, R.M., C.U. and T.M.; writing—review and editing, T.M. and A.H.; supervision, T.M. and A.H.; project administration, T.M. and A.H.; funding acquisition, T.M. and A.H. All authors have read and agreed to the published version of the manuscript.

Funding: This research was funded by a Grant-in-Aid for Scientific Research (Japan Society for the Promotion of Science, Nos. 19H02793, 20H02805).

Institutional Review Board Statement: Not applicable.

Informed Consent Statement: Not applicable.

Data Availability Statement: The data presented in this study are available in the article.

Conflicts of Interest: The authors declare no conflict of interest.

References

1. Wong, T.-S.; Sun, T.; Feng, L.; Aizenberg, J. Interfacial Materials with Special Wettability. *MRS Bull.* **2013**, *38*, 366–371. [[CrossRef](#)]
2. Kota, A.K.; Choi, W.; Tuteja, A. Superomniphobic Surfaces: Design and Durability. *MRS Bull.* **2013**, *38*, 383–390. [[CrossRef](#)]

3. Urata, C.; Masheder, B.; Cheng, D.F.; Miranda, D.F.; Dunderdale, G.J.; Miyamae, T.; Hozumi, A. Why Can Organic Liquids Move Easily on Smooth Alkyl-Terminated Surfaces? *Langmuir* **2014**, *30*, 4049–4055. [[CrossRef](#)]
4. Tsujii, K.; Yamamoto, T. Super Oil-Repellent Surfaces. *Angew. Chem.* **1997**, *36*, 1011–1012. [[CrossRef](#)]
5. Tuteja, A.; Choi, W. Designing superoleophobic surfaces. *Science* **2007**, *318*, 1618–1622. [[CrossRef](#)]
6. Zhang, J.P.; Seeger, S. Superoleophobic Coatings with Ultralow Sliding Angles Based on Silicone Nanofilaments. *Angew. Chem.* **2011**, *50*, 6652–6656. [[CrossRef](#)]
7. Deng, X.; Mammen, L. Candle soot as a template for a transparent robust superamphiphobic coating. *Science* **2012**, *335*, 67–70. [[CrossRef](#)] [[PubMed](#)]
8. Liu, T.L.; Kim, C.J. Turning a surface superrepellent even to completely wetting liquids. *Science* **2014**, *346*, 1096–1100. [[CrossRef](#)]
9. Wei, X.; Hong, S.C.; Lvovsky, A.I.; Held, H.; Shen, Y.R. Evaluation of Surface vs Bulk Contributions in Sum-Frequency Vibrational Spectroscopy Using Reflection and Transmission Geometries. *J. Phys. Chem. B* **2000**, *104*, 3349–3354. [[CrossRef](#)]
10. Mori, F.; Kabashima, S.; Kawakami, T.; Yamamoto, T.; Miyamae, T.; Iimura, K.; Tabori, N. Effect of the interfacial structures of alkyl-side-chain polymer films on the peel force. *Int. J. Adhes. Adhes.* **2018**, *82*, 166–172. [[CrossRef](#)]
11. Tong, Y.; Tyrode, E.; Osawa, M.; Yoshida, N.; Watanabe, T.; Nakajima, A.; Ye, S. Preferential Adsorption of Amino-Terminated Silane in a Binary Mixed Self-Assembled Monolayer. *Langmuir* **2011**, *27*, 5420–5426. [[CrossRef](#)] [[PubMed](#)]
12. Urata, C.; Cheng, D.F.; Masheder, B.; Hozumi, A. Smooth, Transparent and Nonperfluorinated Surfaces Exhibiting Unusual Contact Angle Behavior toward Organic Liquids. *RSC Adv.* **2012**, *2*, 9805–9808. [[CrossRef](#)]
13. Urata, C.; Masheder, B.; Cheng, F.D.; Hozumi, A. How to Reduce Resistance to Movement of Alkane Liquid Drops Across Tilted Surfaces Without Relying on Surface Roughening and Perfluorination. *Langmuir* **2012**, *28*, 17681–17689. [[CrossRef](#)]
14. Miyamae, T.; Tsukagoshi, K.; Matsuoka, O.; Yamamoto, S.; Nozoye, H. Surface Characterization of Polyamic Acid and Polyimide Films Prepared by Vapor Deposition Polymerization by Using Sum-Frequency Generation. *Langmuir* **2001**, *17*, 8125–8130. [[CrossRef](#)]
15. Chiang, C.H.; Ishida, H.; Koenig, J.L. The structure of γ -aminopropyltriethoxysilane on glass surfaces. *J. Coll. Interface Sci.* **1980**, *74*, 396–404. [[CrossRef](#)]
16. Ye, S.; Nihonyanagi, S.; Uosaki, K. Sum frequency generation (SFG) study of the pH-dependent water structure on a fused quartz surface modified by an octadecyltrichlorosilane (OTS) monolayer. *Phys. Chem. Chem. Phys.* **2001**, *3*, 3463–3469. [[CrossRef](#)]
17. Lahorija, B.; Vensa, V.; Vladimir, D. Conformational and vibrational analysis of γ -aminopropyltriethoxysilane. *J. Mol. Struct.* **2007**, *834*, 355–363.
18. Ye, S.; Noda, H.; Nishida, T.; Morita, S.; Osawa, M. Cd^{2+} -Induced Interfacial Structural Changes of Langmuir–Blodgett Films of Stearic Acid on Solid Substrates: A Sum Frequency Generation Study. *Langmuir* **2004**, *20*, 357–365. [[CrossRef](#)]
19. Wang, H.-F.; Gan, W.; Rao, Y.; Wu, B.H. Quantitative Spectral and Orientational Analysis in Surface Sum Frequency Generation Vibrational Spectroscopy (SFG-VS). *Int. Rev. Phys. Chem.* **2005**, *24*, 191–256. [[CrossRef](#)]
20. Tyrode, E.; Liljeblad, J.F.D. Water Structure next to Ordered and Disordered Hydrophobic Silane Monolayers: A Vibrational Sum Frequency Spectroscopy Study. *J. Phys. Chem. C* **2013**, *117*, 1780–1790. [[CrossRef](#)]
21. Liu, Y.; Wolf, L.K.; Messmer, M.C. A Study of Alkyl Chain Conformational Changes in Self-Assembled N-Octadecyltrichlorosilane Monolayers on Fused Silica Surfaces. *Langmuir* **2001**, *17*, 4329–4335. [[CrossRef](#)]
22. Wolf, L.K.; Yang, Y.J.; Pizzolatto, R.L.; Messmer, M.C. Microscopic Structure of Chromatographic Interfaces as Studied by Sum-Frequency Generation Spectroscopy. *ACS Symp. Ser.* **2001**, *781*, 293–305.
23. Offord, D.A.; Griffin, J.H. Kinetic Control in the Formation of Self-Assembled Mixed Monolayers on Planar Silica Substrates. *Langmuir* **1993**, *9*, 3015–3025. [[CrossRef](#)]
24. Pizzolatto, R.L.; Yang, Y.J.; Messmer, M.C. Conformational Aspects of Model Chromatographic Surfaces Studied by Sum-Frequency Generation. *Anal. Chim. Acta* **1999**, *397*, 81–92. [[CrossRef](#)]